

Discovery of a Novel Class of Dual GPBAR1 Agonists–ROR γ t Inverse Agonists for the Treatment of IL-17-Mediated Disorders

Bianca Fiorillo,¹ Rosalinda Roselli,¹ Claudia Finamore,¹ Michele Biagioli,* Cristina di Giorgio, Martina Bordoni, Paolo Conflitti, Silvia Marchianò, Rachele Bellini, Pasquale Rapacciuolo, Chiara Cassiano, Vittorio Limongelli, Valentina Sepe,* Bruno Catalanotti, Stefano Fiorucci, and Angela Zampella



Cite This: *ACS Omega* 2023, 8, 5983–5994



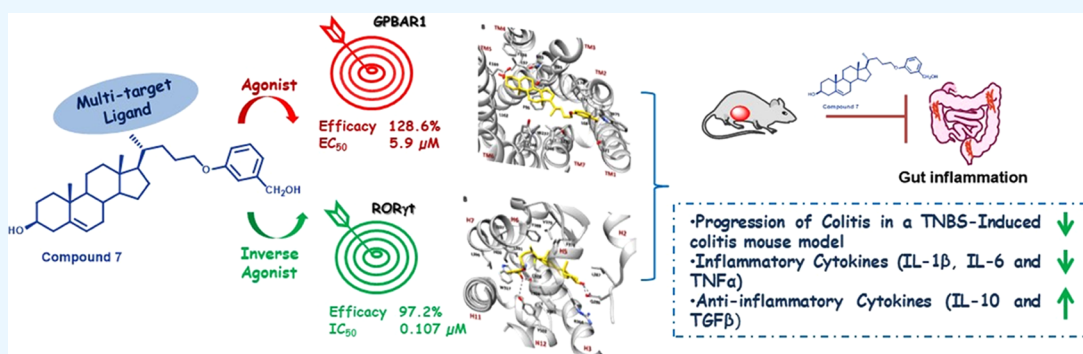
Read Online

ACCESS |

Metrics & More

Article Recommendations

Supporting Information



ABSTRACT: Retinoic acid receptor-related orphan receptor γ -t (ROR γ t) and GPBAR1, a transmembrane G-protein-coupled receptor for bile acids, are attractive drug targets to develop clinically relevant small modulators as potent therapeutics for autoimmune diseases. Herein, we designed, synthesized, and evaluated several new bile acid-derived ligands with potent dual activity. Furthermore, we performed molecular docking and MD calculations of the best dual modulators in the two targets to identify the binding modes as well as to better understand the molecular basis of the inverse agonism of ROR γ t by bile acid derivatives. Among these compounds, 7 was identified as a GPBAR1 agonist (EC₅₀ 5.9 μ M) and ROR γ t inverse agonist (IC₅₀ 0.107 μ M), with excellent pharmacokinetic properties. Finally, the most promising ligand displayed robust anti-inflammatory activity *in vitro* and *in vivo* in a mouse model of 2,4,6-trinitrobenzene sulfonic acid (TNBS)-induced colitis.

INTRODUCTION

Immune cells in the gastrointestinal tract and liver are continuously exposed to microbial antigens generated by the intestinal microbiota. However, because the maintenance of immune homeostasis in enterohepatic tissues is essential to prevent the onset of inflammation, mechanisms that regulate the development of a tolerogenic phenotype by immune cells in the gastrointestinal tract and liver are only partially known.

Bile acids (BAs)¹ are steroidal molecules that represent the end product of cholesterol metabolism, exerting their regulatory function by activating a family of receptors known as the bile acid-activated receptors (BARs). Among these, the farnesoid X receptor (FXR) and the G-protein-coupled bile acid receptor (GPBAR1, also commonly named M-BAR or Takeda G-protein-coupled receptor 5, TGR5) have proven to be druggable, and several selective or dual ligands have been developed.^{2–5} Both FXR and GPBAR1 are expressed by cells of innate immunity, and their activation reverses intestinal and systemic inflammation in a variety of preclinical models.

However, the lack of expression on cells of adaptive immunity limits the development of FXR and GPBAR1 agonists for therapeutic purposes in those settings where T cells play a mechanistic role.⁶ The retinoic acid receptor-related orphan receptors (RORs) represent key regulators of many physiological and pathological processes. Among ROR isoforms, ROR γ is highly expressed in lymphoid organs, skeletal muscles, adipose tissues, kidneys, and liver, and ROR γ t plays a role in regulating T_H17 cells, a subset of T helper lymphocytes whose activation drives intestinal inflammation in IBD patients.^{4,7,8} Additionally, the overexpression of ROR γ t in naive CD4⁺ T cells leads to the induction and development of T_H17 cells, whereas

Received: December 12, 2022

Accepted: January 12, 2023

Published: January 31, 2023



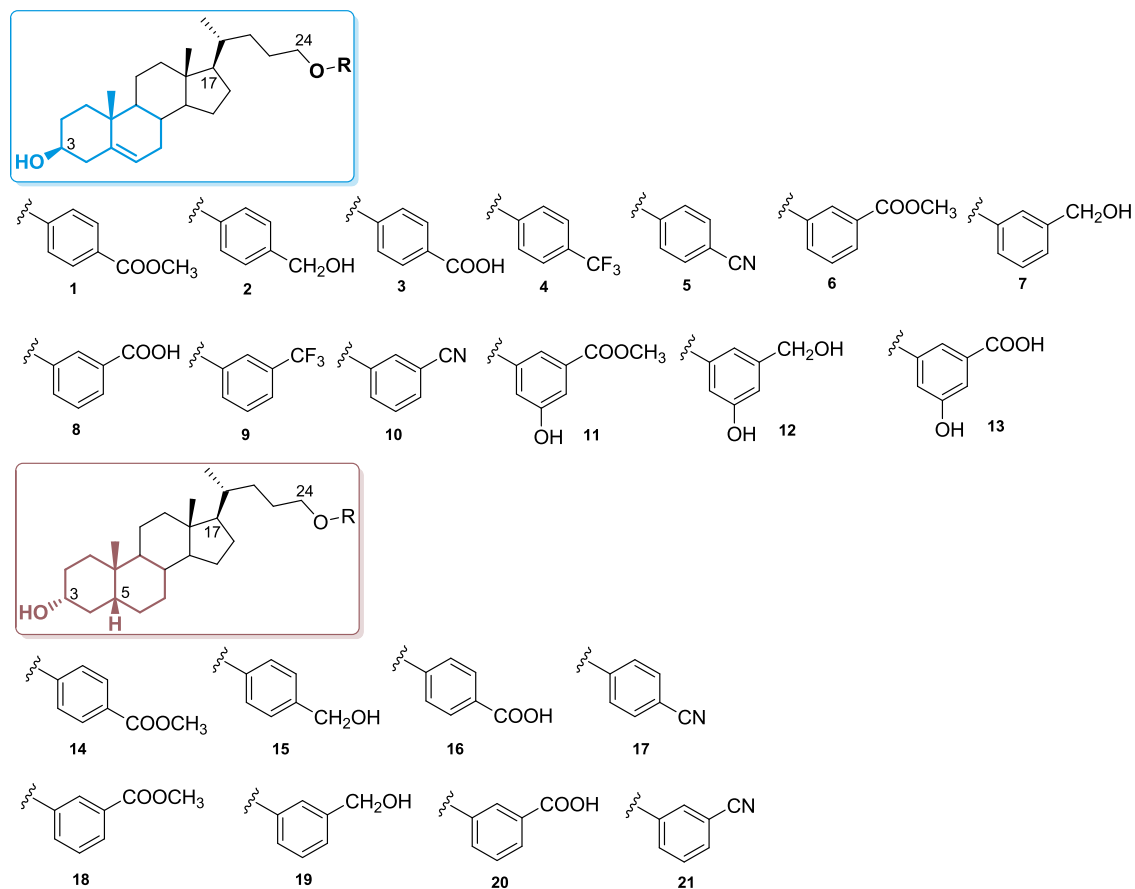


Figure 1. Chemical structure of 1–21.

Scheme 1. Synthesis of Analogues 1–21

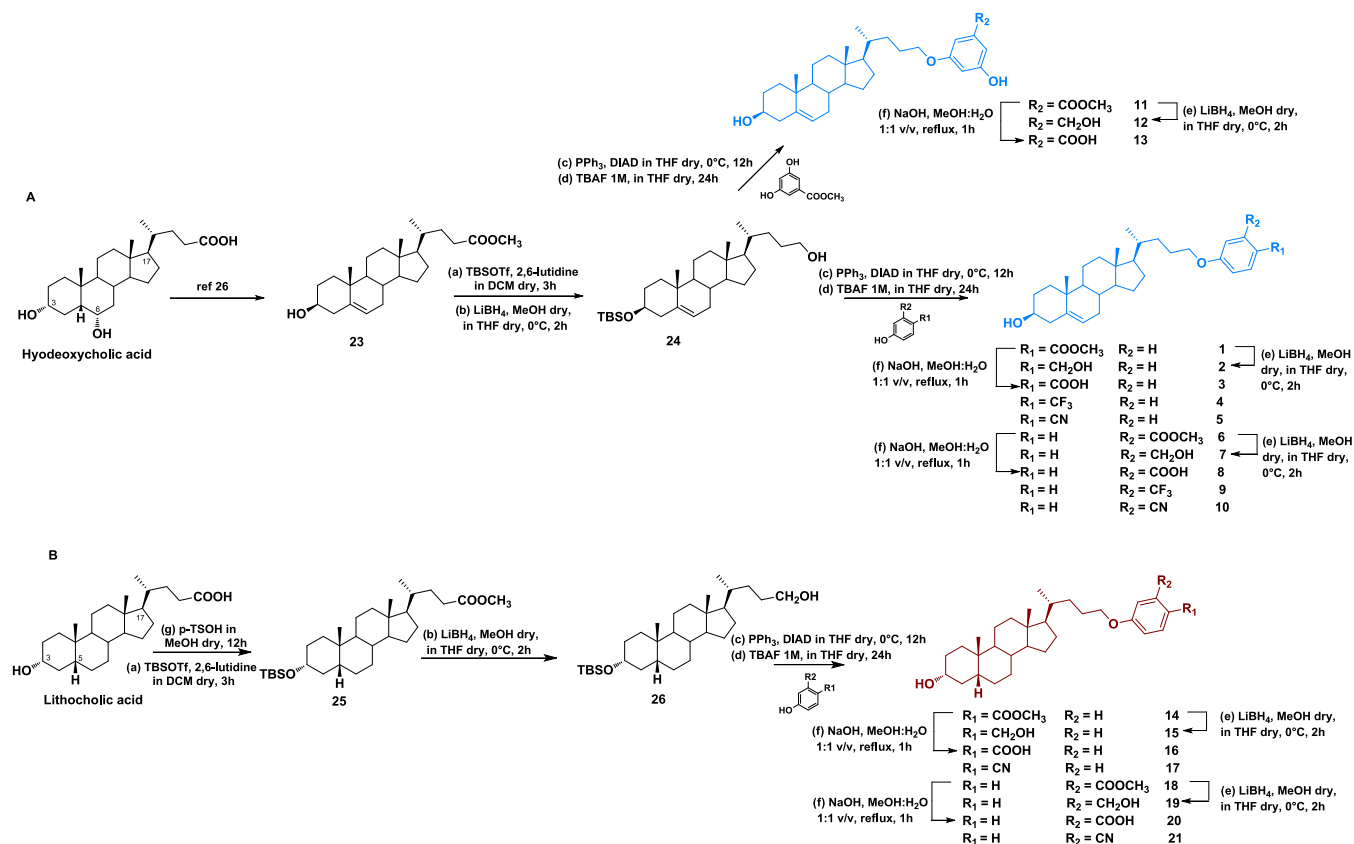
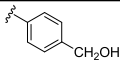
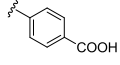
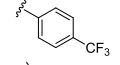
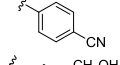
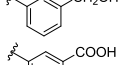
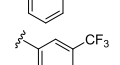
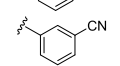
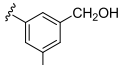
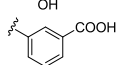
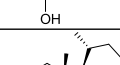
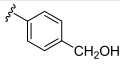
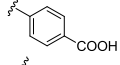
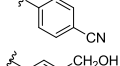
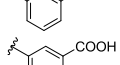
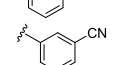
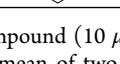


Table 1. Efficacy on GPBAR1 and ROR γ ^{abc}

First subset			
Compd	R	GPBAR1 ^a	ROR γ ^b
2		13.4 ± 10.3	nt ^c
3		44.3 ± 0.5	95.6 ± 1.8
4		21.8 ± 6	nt ^c
5		41.1 ± 12	72.5 ± 2.9
7		128.6 ± 14.4	97.2 ± 3.6
8		16.8 ± 8.3	nt ^c
9		17.9 ± 0.2	nt ^c
10		20.3 ± 4.3	nt ^c
12		32.7 ± 5.9	nt ^c
13		26.3 ± 1.1	nt ^c
Second subset			
Compd	R	GPBAR1 ^a	ROR γ ^b
15		114.1 ± 0.04	52.6 ± 9.2
16		42.6 ± 0.5	10.2 ± 6.7
17		57.1 ± 1	70.1 ± 3.5
19		96.2 ± 5.9	48.0 ± 10.2
20		45.2 ± 7.8	54.9 ± 7.7
21		86.1 ± 1.8	54.3 ± 7.2

^aEff. (%) is the maximum efficacy of the compound (10 μ M) relative to TLCA (10 μ M) as 100 in transactivation of a cAMP-responsive element (CRE) on HEK-293T cells; results are the mean of two experiments \pm SD. ^bEff. is the efficacy of the compound (10 μ M) as % of inhibition calculated from the residual activity of ROR γ , defining the wells containing only vehicle (DMSO) as 100% control and the wells without the protein as 0% control. ^cnt means not tested.

its inhibition reduces the autoimmune response^{4,9} and holds promise in the treatment of colitis, autoimmune diseases, and metabolic disorders.^{8,10} Several cholesterol intermediates and metabolites exhibit high affinity toward ROR γ and act as agonists or inverse agonists.^{11,12} The mechanism of action of ROR γ agonists is explained through the stabilization of the H-bond between His479 and Tyr502 on Helix 11 (H11) and Helix 12 (H12), respectively, allowing the recruitment of transcriptional coactivators on target genes. On the other hand, inverse agonists of ROR γ disrupt the H-bond between H11 and H12 through a mechanism of interaction that includes Leu324,

Trp317, His479, and Tyr502, preventing the recruitment of transcriptional coactivators and inhibiting T_H17 cell differentiation both *in vitro* and *in vivo*.^{13–18}

The specific structural motifs of ROR γ inverse agonists rely on the presence of a hydrogen bond acceptor at one end of the molecule and a lipophilic and rigid motif on the other side, appropriately spaced.^{17,19} ROR γ cocrystallized structures demonstrated that the AF-2 domain at the C-terminus of the receptor, together with helices H3, H4, and H5, forms a charge clamp pocket that facilitates the binding of coactivators. Mutagenesis studies of this region confirmed that such a

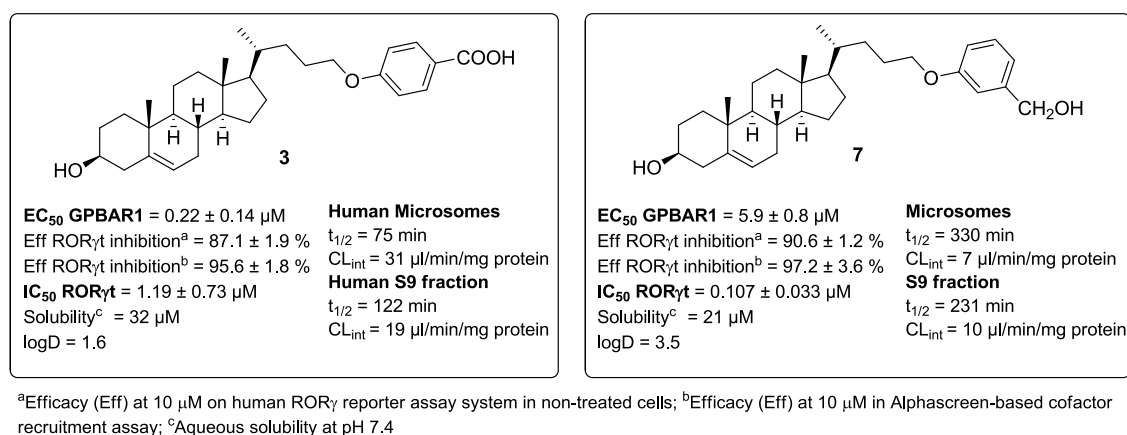


Figure 2. *In vitro* assays. An overview of the efficacy, potency, and preliminary PK parameters of compounds 3 and 7.

charged clamp pocket is required for hydroxycholesterols to affect ROR γ t activity.¹⁴

While ROR γ t expression is limited to T_H17 cells and innate lymphoid 3 cells (ILC3s), GPBAR1 is expressed by the cells of innate immunity, therefore developing dual ROR γ t antagonists/GPBAR1 agonists might provide a unique opportunity to simultaneously target the innate immunity along with effector mechanisms in the T_H17 pathway, tightening the spectrum of activity and limiting the potential side effects linked to the nonselective inhibition of the whole immune system.^{5,20–25}

Building on this background,²³ we have designed a new series of bile acid-derived ligands with potential multitarget activity (compounds 1–21, Figure 1). Synthesis, pharmacological profiling, and computational studies resulted in the discovery of 3 and 7 as GPBAR1 agonists and ROR γ t inverse agonists. Further, the excellent pharmacokinetic profile of 7 placed this novel hybrid ligand in a privileged position for preclinical studies, and deep *in vivo* pharmacological evaluation demonstrated its therapeutical potential in the treatment of colitis. Therefore, here, we present, in a proof-of-concept study, the first evidence that dual modulation of ROR γ t/GPBAR1 represents a new armamentarium in IBD pharmacological treatment.

RESULTS AND DISCUSSION

Starting from hydoxycholeic acid and lithocholic acid, two different subsets of compounds, focusing on the ring A and B junction and modifying the side chain in length and in the nature of the end-group, have been prepared (Figure 1).

The preparation of subset 1 (compounds 1–13, Scheme 1) was obtained from compound 23²⁶ by alcohol protection at C3 and reduction at the side-chain methyl ester to give 24, which was used in multiple Mitsunobu reactions with various phenols (Scheme 1) to produce, after deprotection at C3, derivatives 4, 5, 9, and 10 and the expected methyl esters (1, 6, and 11).²⁷ Finally, LiBH₄ reduction and basic hydrolysis afforded the corresponding alcohols (compounds 2, 7, and 12) and carboxylic acids (compounds 3, 8, and 13), respectively.

For the synthesis of the second subset of compounds (14–21), lithocholic acid was used as a starting material. To enhance the selectivity of the Mitsunobu coupling at C24,²⁸ we protected the C3 alcoholic function before LiBH₄ reduction of ester in the side chain. Intermediate 26 was coupled with four different phenols to produce 14, 17, 18, and 21. LiBH₄ reduction and basic hydrolysis on methyl esters 14 and 18 furnished the

alcohols 15 and 19 and the carboxylic acids 16 and 20, respectively.

A selection of new derivatives (compounds 2–5, 7–10, 12, 13, 15–17, and 19–21) was first tested in the luciferase reporter assay on HEK-293T cells transfected with GPBAR1. Particularly, we decided to exclude from our assays the ester derivatives (compounds 1, 6, 11, 14, and 18) because of their tendency to be hydrolyzed *in vivo*. Results of these assays, reported in Table 1, revealed that several compounds exhibited good efficacy as GPBAR1 agonists and, notably, 7, 15, and 19 showed similar activity to tauroolithocholic acid (TLCA), the most potent endogenous GPBAR1 agonist.

All of the compounds showing an efficacy greater than 40% were further analyzed on ROR γ t to identify new tools for the treatment of IBD.

To evaluate inverse-agonist activities against human ROR γ t of the selected compounds, the human ROR γ reporter assay system was used. Moreover, the ability of these compounds to interfere with the ROR γ t-SRC-1 interaction was also evaluated in a cell-free α -screen assay. The efficacies of all tested compounds (3, 5, 7, 15–17, and 19–21) are reported in Table 1. Notably, apart from 17, all compounds of the second subset, endowed with the bile acid shape (*cis* A/B ring junction), showed lower efficacy against ROR γ t than the corresponding derivatives belonging to the first subset, with 3, 5, and 7 showing the best efficacy on ROR γ t. Compounds 5 and 17 resulted in being less soluble in aqueous buffers (10 and 15 μM, respectively), thus hampering further pharmacological evaluations and prompting us to investigate the most promising compounds, 3 and 7.

As reported in Figure 2, 3 and 7 exhibited good activity against both receptors, representing the best match in terms of efficacy and potency. These compounds exerted a concentration-dependent effect on the activation of CREB in HEK-293T cells transfected with GPBAR1 with an EC₅₀ of 0.22 and 5.9 μM, respectively. Despite the low value of EC₅₀ for 3, it should be considered that the above potency is related to an efficacy of about 44% when compared to TLCA (Table 1), whereas the efficacy of 7 was about 129%. Moreover, 3 and 7 inhibited the binding of ROR γ t-LBD to coactivator peptide SRC-1 with an IC₅₀ of 1.19 and 0.107 μM, respectively. The potency of 7 was also confirmed in the human ROR γ t reporter assay, revealing an IC₅₀ of 0.193 μM. Ursolic acid and digoxin were used as the assay control (IC₅₀ values of 0.116 and 0.237 μM, respectively). Moreover, both compounds exhibited excellent selectivity with

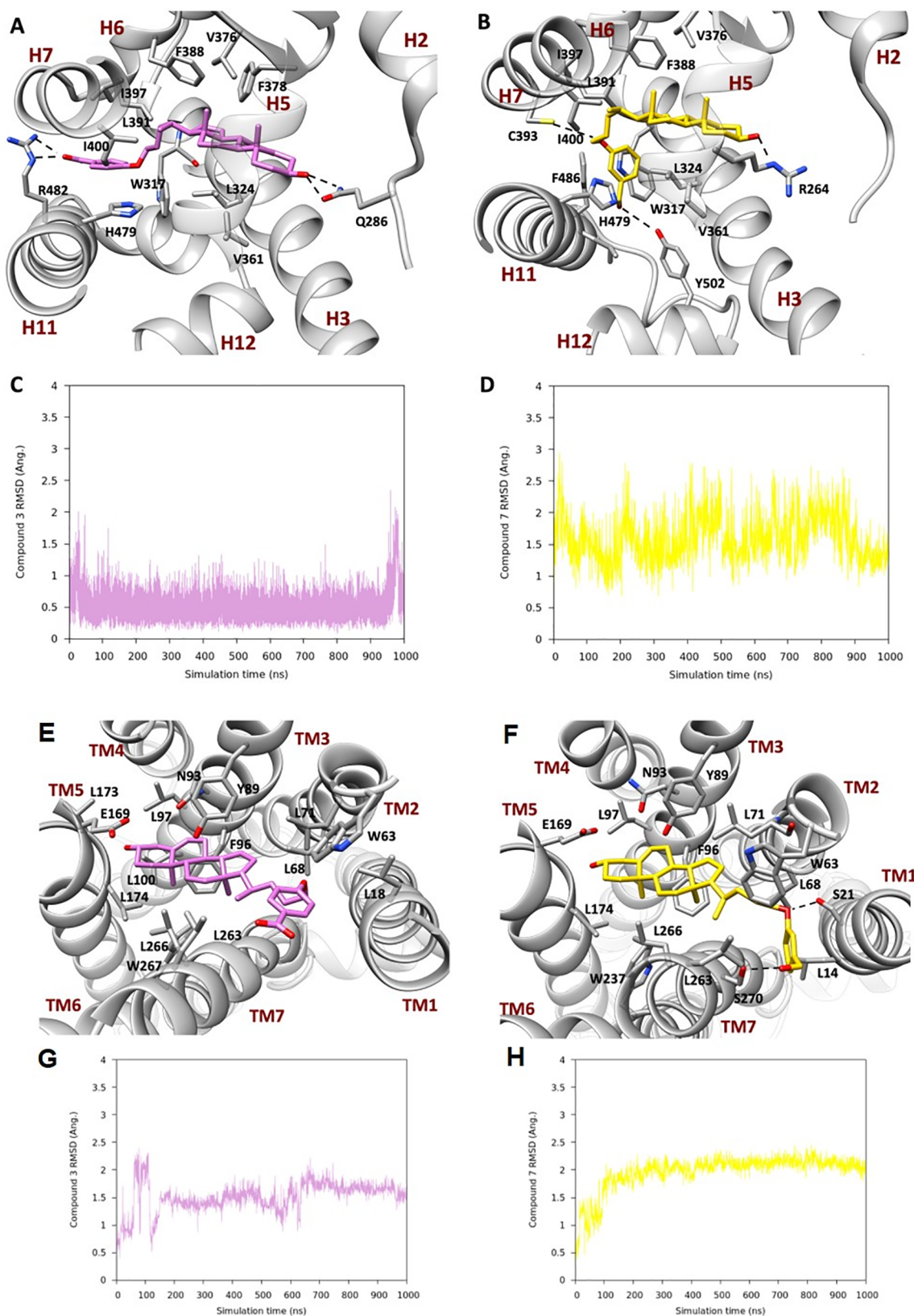


Figure 3. Representation of the MD binding mode of (A) 3 and (B) 7 in ROR γ and (E) 3 and (F) 7 in the GPBAR1 homology model. The ligands are represented as *pink* and *gold* sticks, respectively, and the interacting residues of the receptor are shown in *gray* and labeled, with oxygen atoms in *red* and nitrogens in *blue*. The receptor is represented as ribbons with its helix labeled. Hydrogens are omitted for the sake of clarity and H-bonds are displayed as dashed lines. Plots of average RMSD calculated on the heavy atoms of the steroidal scaffold of (C) and (G) 3 and (D) and (H) 7.

no off-target activity toward metabolic nuclear receptors, such as FXR, LXR α , and LXR β (Table S1 in the SI).

Compounds 3 and 7 were further investigated to assess their aqueous solubility, LogD, and the liability to hepatic

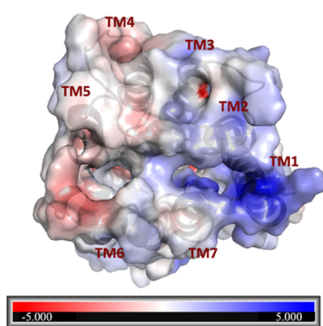


Figure 4. Electrostatic potential map calculated on GPBAR1. The surface is colored according to the electrostatic potential, where the red color (negative potential) indicates an excess of negative charges and the blue color (positive potential) is an excess of positive charges. The white regions correspond to fairly neutral potentials. The values are expressed in atomic units (a.u).

metabolizing enzymes (Figure 2). Both the liver microsomal fraction and S9 fraction were employed. The compounds resulted in being sufficiently soluble in an aqueous buffer at pH 7.4 and were endowed with proper LogD values. Moreover, *in vitro* treatment with human liver microsomes and human liver S9 fractions demonstrated a very promising $t_{1/2}$ value of 330 min ($CL_{int} = 7 \mu\text{L}/\text{min}/\text{mg}$ protein) for compound 7. All of these data highlight the pharmacological potential of 7 in associating potency and efficacy in the dual modulation of ROR γ t and GPBAR1 with excellent metabolic stability.

Computational Studies. To elucidate the binding mode of the most promising dual-activity derivatives, 3 and 7, toward ROR γ t and GPBAR1, molecular modeling studies based on docking and MD calculations, which are widely employed techniques to study ligand/protein binding interactions,^{29–31} have been carried out. First, we performed molecular docking calculations using the Glide software package (SI).³² As the starting structure, the human crystallographic structure of the active conformation of the ROR γ t-LBD domain with PDB ID 3l0j³³ was employed. For the GPBAR1 receptor, we used the 3D model developed in 2014.³⁴ The docking calculations identified binding modes of 3 and 7 to ROR γ t and GPBAR1 (SI Figures S1

and S3) in agreement with those previously reported for structurally similar ligands.³³ To assess the docking results in a more realistic condition, where protein flexibility and the water effect are taken into account, the best docking pose for both 3 and 7 underwent a 1 μs MD simulation in ROR γ t in an explicit solvent. The results showed that, after a few ns of simulation, 3 underwent a conformational rearrangement with respect to the initial docking pose (Figure 3, panels A and C), leading to an extended conformation of the flexible chain at C-17, while the hydroxyl group at C-3 kept a stable H-bond with the Gln286 side chain on H2 as found by docking. The steroidal scaffold was placed in the amphipathic pocket between H4 and H5, where it was further stabilized by a set of hydrophobic interactions established with the side chains of Leu324, Val361, Val376, and Phe378. The aromatic ring was located between H4 and H11, where it took part in aromatic interactions with Trp317 and His479. The carboxyl group on the ligand side chain moved during the MD simulation to form an H-bond with Arg482 located on H11 (Figure 3, panel A). Finally, the above conformational change and the stacking interaction between the aromatic ring in the ligand's side chain and the side chain of His479 caused the destruction of the H-bond between His479 and Tyr502 and a slight shift of H12, altering the binding site of the coactivator (SI Figure S4).

At the end of the production run of 7, the ligand's binding mode was stabilized by different interactions (Figure 3, panels B and D). The hydroxyl group at C-3 H-bonded Arg264, whereas the steroidal scaffold was stabilized by hydrophobic interactions with Leu324, Val361, Val376, and Phe388. The methylene linker on the side chain at C-17 interacted with Leu391, Ile397, and Ile400, whereas the ethereal oxygen H-bonded Cys393. Finally, the aromatic ring was stabilized between H7 and H11 by aromatic interactions with Trp317, His479, and Phe486. A direct interaction of the 7 side chain with Tyr502 caused a more marked weakening of the H-bond network between His479 and Tyr502 (SI Figure S4), stabilizing the open form of H12, which hampered the recruitment of the coactivator. Our results agree with the available literature data,¹¹ showing that the mechanism of the action of inverse agonists relies on the disruption of the H-bond between His479 and Tyr502. This event destabilizes the

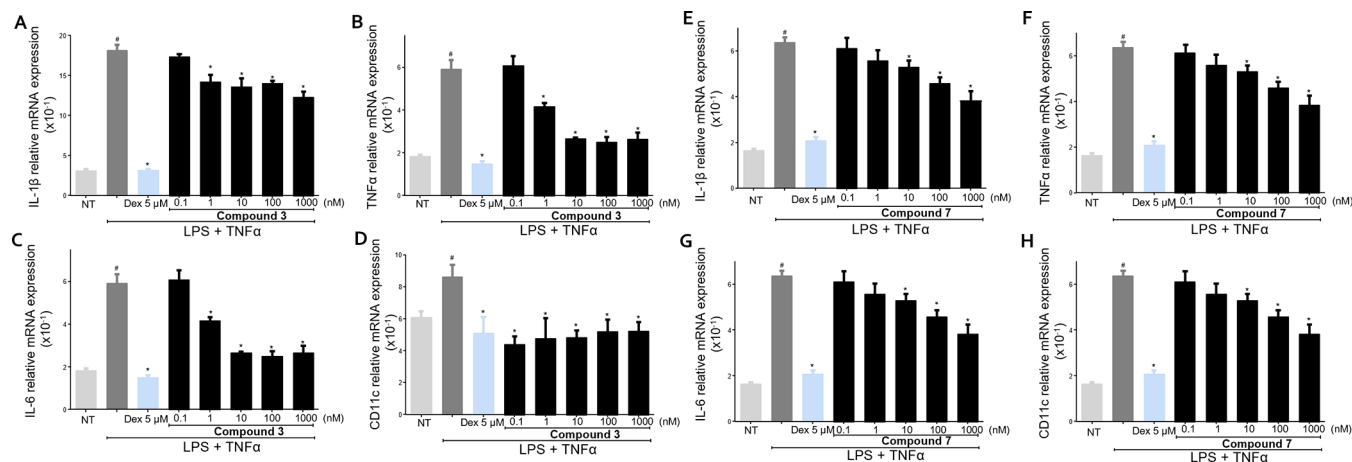


Figure 5. U937 cells activated with LPS (100 ng/mL) plus TNF α (100 ng/mL) for 24 h, alone or in combination with 3 or 7 at 0.1, 1, 10, 100, and 1000 nM. Dexamethasone (Dex) was used at 5 μM . Quantitative real-time PCR analysis of the expression of proinflammatory genes IL-1 β (A and E), TNF α (B and F), IL-6 (C and G), and M1 marker CD11c (D and H). These data are normalized to TBP mRNA expression. Data are derived from five replicates. Results represent the mean \pm SEM. # $p < 0.05$ vs NT group and * $p < 0.05$ vs LPS plus TNF α group. Analysis of variance (ANOVA) was used for statistical comparisons.

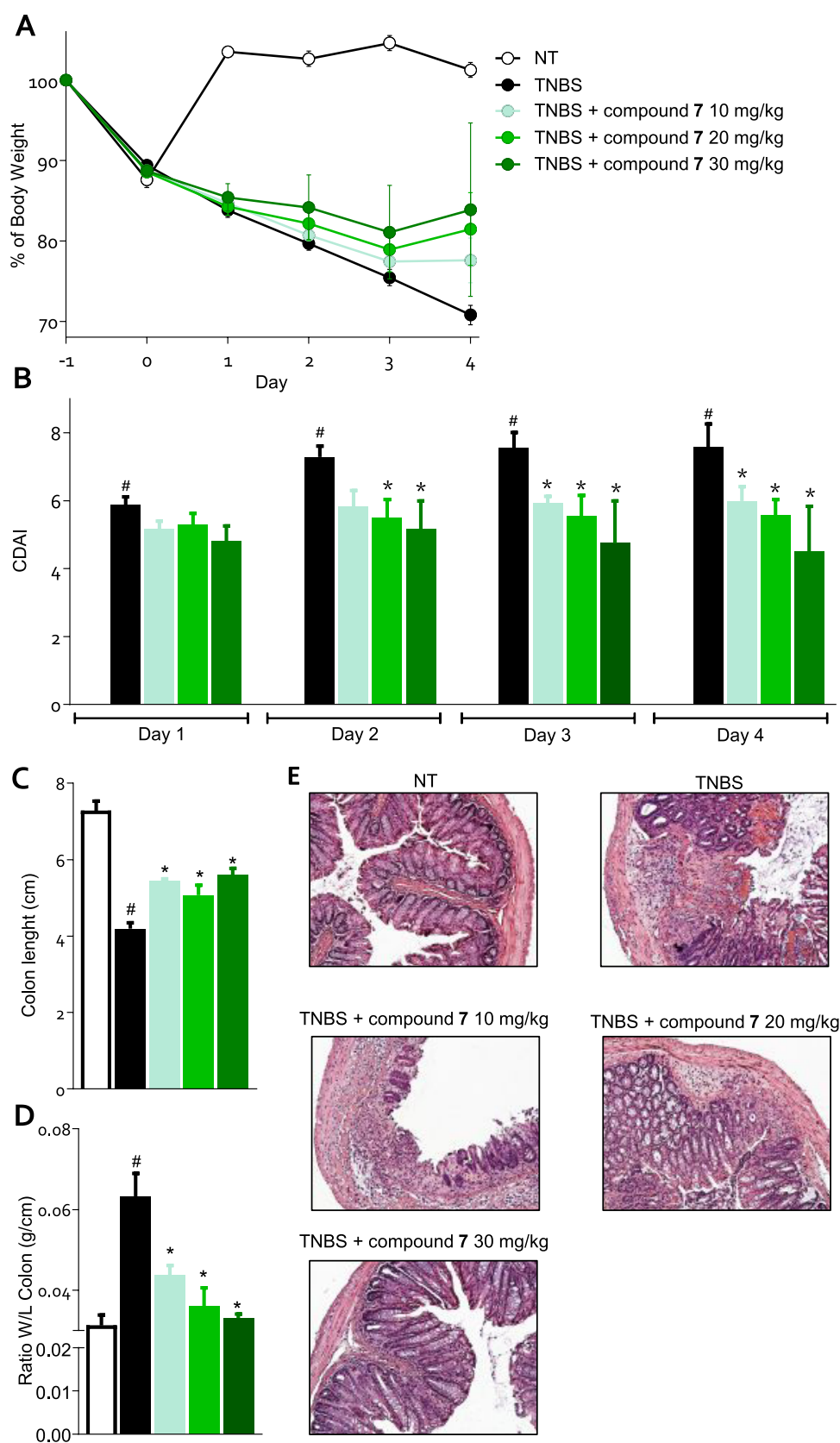


Figure 6. Mice treated with TNBS were administered with the vehicle or 7 at doses of 10, 20, or 30 mg/kg/day by gavage from day 0 to day 4. (A) Change in body weight, (B) CDAI score, (C) colon length, (D) ratio between colon weight and colon length, (E) H&E staining on colon sections of the control, TNBS-treated, and TNBS plus various concentrations of 7 treated mice. Results are the mean \pm SEM of 5–10 mice per group. * p < 0.05 vs TNBS group and # p < 0.05 vs NT group.

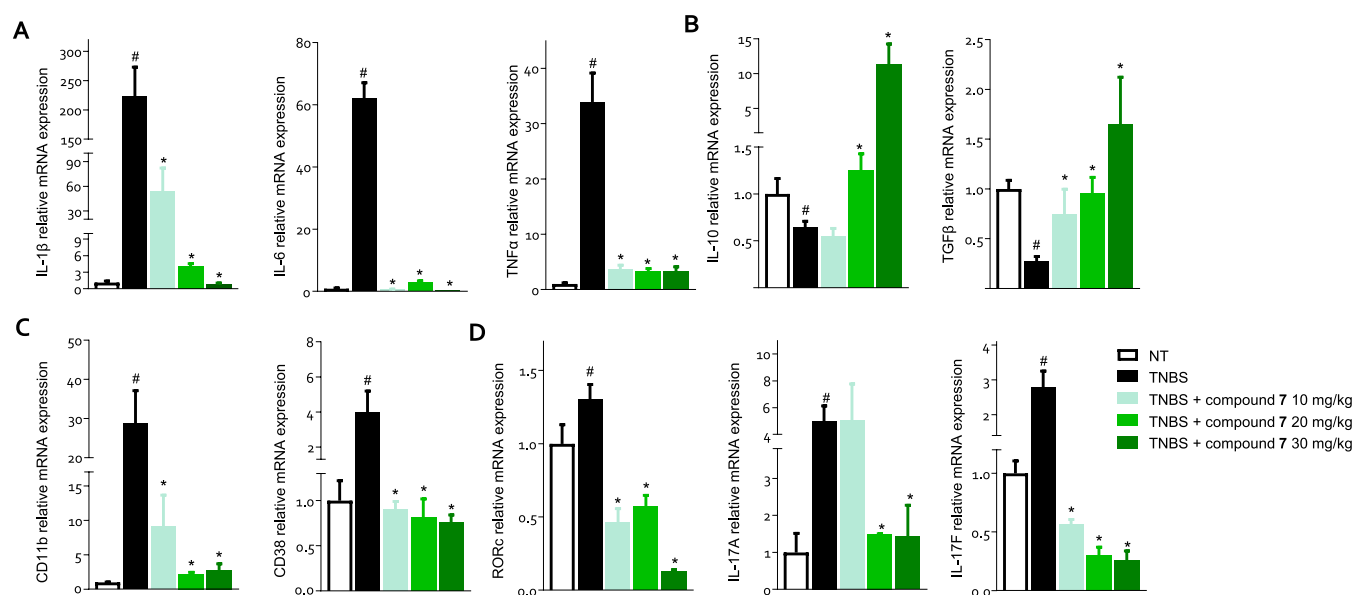


Figure 7. C57 male mice treated with TNBS were administered with the vehicle or 7 at doses of 10, 20, or 30 mg/kg/day by gavage from day 0 to day 4. The relative mRNA expression of (A) proinflammatory (IL-1 β , IL-6, and TNF α) and (B) anti-inflammatory cytokines (IL-10 and TGF β), (C) macrophage markers, and (D) T_H17 cell markers in the colon assayed by RTPCR. Data are normalized to the expression of *Gapdh*, *Tbp*, and *Actb* mRNA. Results are the mean \pm SEM of 5–10 mice per group. * p < 0.05 vs TNBS group and # p < 0.05 vs NT group.

active form of the receptor and hampers the recruitment of the transcriptional coactivator SRC.

During the MD simulations, both the ligands showed the so-called “push–pull” mechanism of action, *i.e.*, pushing Trp317 and pulling H479 or Y502, already proposed for other inverse agonists.^{17,18} In more detail, the ligands induced a flip of W317 into a position that did not allow the H-bond interaction between His479 and Thr502, while interacting with one of such residues. As the final effect, the tertiary structure of H11–12 is perturbed, thus affecting the recruitment of the coactivator and target gene expression (SI Figure S4). Overall, our MD simulations indicated that 3 and 7 work as ROR γ t inverse agonists.

To further evaluate the capability of 3 and 7 to act as inverse agonists, we also performed 500 ns of MD simulations of the cocrystallized agonist ligand, 22*R*-hydroxycholesterol, in the active form of ROR γ t (PDB ID 3l0j).³³ At variance with compounds 3 and 7, the agonist stabilizes the active conformation of ROR γ t (see Figures S4 and S5 and the Supporting Information for details).

In addition, 1 μ s MD calculations were performed on the docking binding modes of 3 and 7 to GPBAR1. After 150 ns, 3 underwent a change in its binding mode, which was then maintained until the end of the simulation (Figure 3, panel G). The hydroxyl group at C-3 was still forming an H-bond with the Glu169 backbone, and the steroidal scaffold was located between transmembrane helices (TM) 3 and 5, formed by Tyr89, Asn93, Phe96, Leu97, Leu174, Leu263, Leu266, and Trp267 and stabilized by hydrophobic interactions. The aromatic ring on the side chain was also involved in hydrophobic interactions with Leu18, Leu68, and Leu71 and in a t-shaped π -stacking with Trp63 (Figure 3, panel E).

Compound 7 binding mode changed after 100 ns of MD (Figure 3, panel H) to achieve a more stable conformation, like the one described for 3. The steroidal scaffold was in the same pocket of 3, and it established hydrophobic interactions with the side chain of several residues, such as Leu14, Trp63, Leu68,

Leu71, Leu97, Leu174, Leu263, Leu266, and Trp267, and H-bonds between the *meta*-CH₂OH group and Ser267 (Figure 3, panel F), the hydroxyl group at C-3 and the backbone of Glu169, and the ethereal oxygen and the side chain of Ser21 that further contributed to stabilize compound 3 in the binding pocket.

The higher affinity of 3 than 7 (Figure 2) can be explained through the electrostatic potential surface calculated on GPBAR1 (Figure 4), where the charge distributions of the binding pocket showed the preference to accommodate 3, which is negatively charged.

In Vitro Pharmacological Evaluation. We have first investigated whether 3 and 7 modulate the inflammatory response of U937 cells, a human monocytic cell, to lipopolysaccharide (LPS) and TNF α . Cells were cocultured with or without compounds at 0.1, 1, 10, 100, and 1000 nM and dexamethasone (Dex) at 5 μ M was used as a control (Figure 5).

Exposure of U937 to LPS *plus* TNF α induced an increase in the production of proinflammatory cytokines IL-1 β , TNF α , and IL-6, also increasing the expression of CD11c, a specific marker of the proinflammatory M1 subtype of macrophages (Figure 5). Compound 3 reduced the expression of proinflammatory cytokines and CD11c. At the highest concentration of 1 μ M, a reduction in the expression of all measured genes was observed by 30–50% compared to cells exposed only to LPS *plus* TNF α (Figure 5). Also, 7 (Figure 5) reverted the inflammatory state induced in U937 cells by LPS *plus* TNF α by reducing the expression of all proinflammatory markers measured with a concentration-dependent effect (Figure 5).

Therefore, 3 and 7 showed comparable immunomodulatory activity *in vitro*, but the data shown in Figure 2 indicated a much higher metabolic stability for 7 compared to 3 with a very high $t_{1/2}$ value. For these reasons, we focused our attention on 7 in the subsequent study *in vivo*.

The effect exerted by 7 was tested in a mouse model of TNBS-induced colitis. The severity of colitis was relieved by 7 in a dose-dependent manner, as demonstrated by the trend in the percentage of body weight and the colitis disease activity index

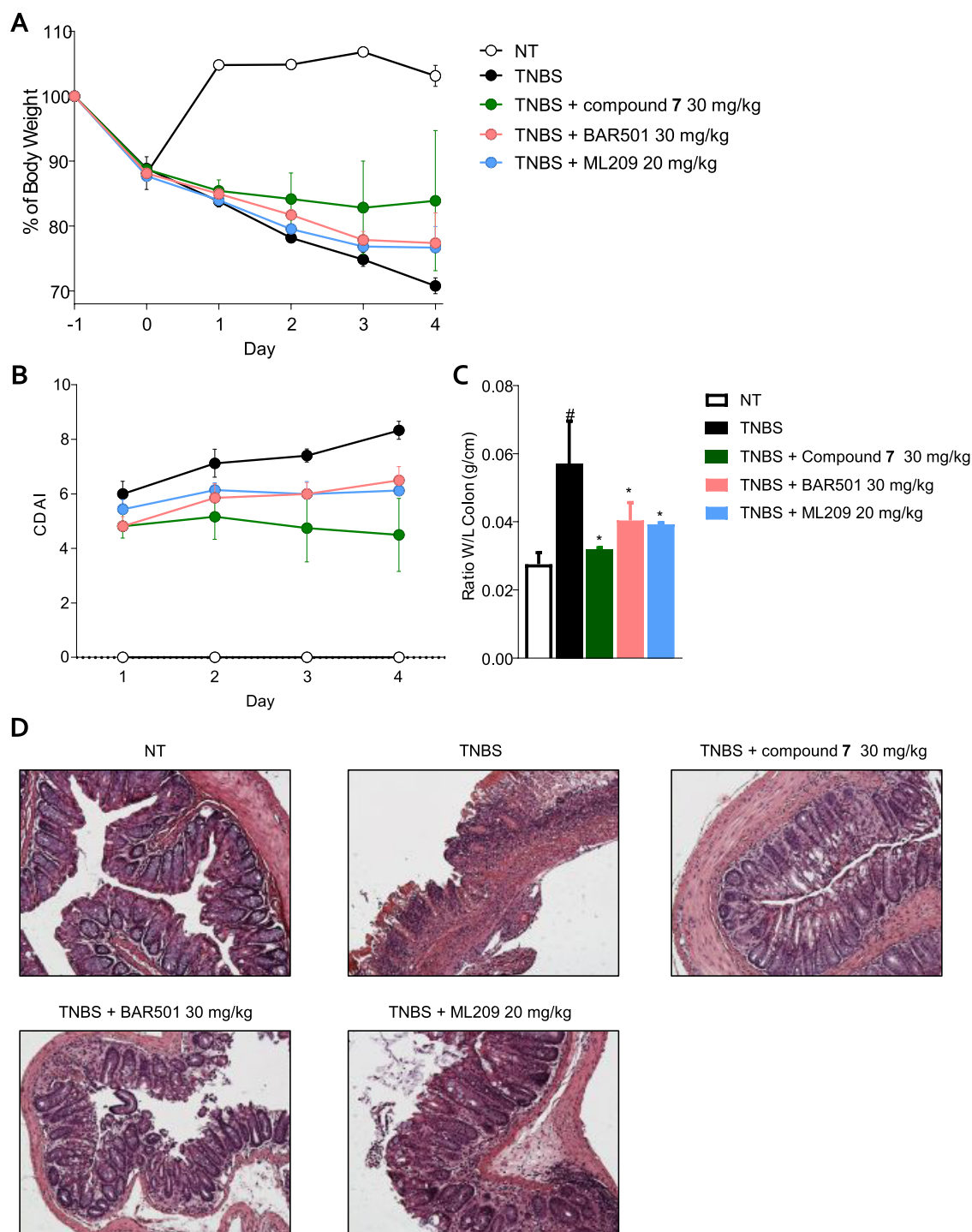


Figure 8. Mice treated with TNBS were administered with the vehicle or 7 30 mg/kg/day, BAR501 30 mg/kg/day, and ML209 20 mg/kg/day by gavage from day 0 to day 4. (A) Change in body weight, (B) CDAI score, (C) ratio between colon weight and colon length, and (D) H&E staining on colon sections of each experimental group. Results are the mean \pm SEM of 5–8 mice per group. * $p < 0.05$ vs TNBS group and [#] $p < 0.05$ vs NT group.

(CDAI) (Figure 6, panels A, B). All three doses of 7 decreased the damage to the colon as demonstrated by both the macroscopic analysis (Figure 6, panels C, D) and the histological analysis using H&E staining (Figure 6, panel E).

To gain deeper insight into the immunomodulatory effect exerted by 7, we have investigated the expression of various cytokines and immune cell markers in the colon of mice rendered colitic by TNBS administration (Figure 7). The development of colon inflammation in this model is associated

with a robust induction in the expression of the proinflammatory cytokines, IL-1 β , IL-6, and TNF α (Figure 7, panel A), along with a downregulation of the anti-inflammatory cytokines IL-10 and TGF β (Figure 7, panel B). Furthermore, TNBS colitis results in robust recruitment in the colon lamina propria of various leukocyte subsets including macrophages and T_H17 lymphocytes.

Treating mice with TNBS induced a strong increase in the colonic expression of CD11b, a macrophage marker (Figure 7,

panel C), suggesting an influx of monocytes into the inflamed tissue. These cells showed a proinflammatory signature, an M1 phenotype, as evidenced by the upregulation of the CD38 gene (Figure 7, panel C). The analysis of the expression of *Rorc*, the gene encoding ROR γ t, and of IL-17A and F demonstrated a robust inflow of T_H17 ROR γ t⁺ cells in the lamina propria of colitis mice (Figure 7, panel D). Compound 7 reverted this inflammatory pattern in a dose-dependent manner and also promoted a strong increase in the expression of IL-10, a potent anti-inflammatory mediator, which represents one of the mechanisms underlying the anti-inflammatory effect of GPBAR1 activation (Figure 7, panels A, B).³⁵ The administration of 7 blunted the inflow of macrophages into the lamina propria of the colon, as demonstrated by the downregulation of CD11b, and reversed the polarization toward the proinflammatory M1 phenotype, as assessed by the decreased expression of CD38 (Figure 7, panel C). On adaptive immunity, the administration of 7 decreased the expression of *Rorc*, IL-17A, and F, negatively modulating the immune response of T_H17 lymphocytes (Figure 7, panel D).

Together, these data support the notion that 7 might represent a promising candidate for the drug therapy of IBD thanks to its ability to modulate both the innate immune response by acting on macrophages and adaptive immunity by inhibiting the polarization/activation of T_H17 lymphocytes.³³

To further investigate the role of simultaneous modulation of ROR γ t and GPBAR1 in protecting against the development of colitis, TNBS-treated mice were force-fed with 7, BARS01, a selective GPBAR1 agonist,³⁶ or ML209, a ROR γ t inverse agonist (Figure 8).³⁷ All three compounds attenuated the development of colitis, highlighting the role of both receptors in the model. Accordingly, compound 7 exerted a greater protective effect than the two selective agents, as demonstrated by the attenuation of the CDAI score, measurement of colon length, and histological damage (Figure 8, panels A–D).

CONCLUSIONS

The present study reports the discovery of a family of new steroidal derivatives acting as GPBAR1 agonists and ROR γ t inverse agonists that might be suitable for the treatment of autoimmune disorders. Our results highlighted a different profile activity of the two series described in the study, driven by the shape of the steroidal scaffold. The cholesterol derivatives (first subset) resulted in being more prone to bind ROR γ t, while on the contrary, the steroidal scaffold of the second subset (bent shape-BAs-like) exhibited better activity toward GPBAR1. Docking studies suggested that the nonplanar structure of the steroidal scaffold of compounds belonging to the second subset could bind the ROR γ t binding pocket after a rotation of the steroidal core, determining the weakening of the network of hydrophobic interactions, the loss of the H-bond of the 3-hydroxyl group to Gln286, and forcing the side chain in a more hindered and apolar region. As regards the second subset, it should be noted that all compounds belong to the LCA scaffold with modification in the carboxylic acid on the side chain, and the results on compound 17, discarded for its low solubility, are consistent with the inhibition of ROR γ t transcriptional activity previously reported for gut microbiota-LCA metabolites (mainly 3-oxo-LCA),^{38,39} suggesting that it is also possible to exploit the bile acid scaffold to design dual GPBAR1 agonists and ROR γ t inverse agonists. Moreover, molecular dynamics simulations showed that the flexibility of the side chain at C17 played a key role in assuming the right conformation to bind

both GPBAR1 and ROR γ t binding pockets, allowing the interaction of the aromatic ring of compounds 3 and 7 to the key residues involved in the receptor activation, Glu169 and Ser20 in GPBAR1, or deactivation, Trp379, His479 and Tyr502 in ROR γ t.

Results from pharmacokinetics analysis revealed that 7 was endowed with excellent metabolic stability, thus deploying the newly hybrid ligand designed for simultaneous modulation of GPBAR1 and ROR γ t in a privileged position to enter preclinical studies.

Data on *in vitro* experiments showed that the activation of GPBAR1 by 7 modulates the polarization of monocytes by blocking the differentiation toward the proinflammatory M1 phenotype and the production of proinflammatory cytokines, counteracting the proinflammatory effect exerted by LPS *plus* TNF α .

Of interest is the effect of 7 in a mouse model of colitis induced by TNBS, showing that 7 relieved signs and symptoms of colitis in a dose-dependent manner, protecting, at 30 mg/kg dose, from weight loss and reduced colon inflammation. Further analysis of colonic cytokines and immune cell markers showed that the beneficial effect of 7 was due to a profound modulation of both innate and adaptive immune responses. In fact, treating mice with 7 reduced the expression of CD38, a specific marker for M1 macrophages, a proinflammatory subset of intestinal macrophages, along with *Rorc*, a marker for T_H17 lineage, indicating a reduction of these two cell populations in the colon's lamina propria. The beneficial effect exerted on macrophages and T_H17 cells led to a consequent reduction in the expression of the proinflammatory cytokines produced by these cells resulting in reduced inflammation in the colon.

In summary, in the present study, we describe the synthesis, the *in vitro* and *in vivo* pharmacological characterization, and the structural requisites of the ligand–receptor interaction of a novel family of cholesterol derivatives including potent dual modulators of ROR γ t/GPBAR1. This study resulted in the identification of compound 7, the first example of a potent GPBAR1 agonist and ROR γ t inverse agonist, that effectively reverts colitis in a validated mouse model of IBD.

ASSOCIATED CONTENT

Supporting Information

The Supporting Information is available free of charge at <https://pubs.acs.org/doi/10.1021/acsomega.2c07907>.

Docking calculations, Figures S1–S5, experimental procedures, ¹H NMR spectra of compounds 1–21 (Figures S6–S26), and HPLC traces of compounds 3 and 7 (Figures S27 and S28) (PDF)

AUTHOR INFORMATION

Corresponding Authors

Michele Biagioli – Department of Medicine and Surgery, University of Perugia, I-06132 Perugia, Italy; Email: michele.biagioli@unipg.it

Valentina Sepe – Department of Pharmacy, University of Naples “Federico II”, I-80131 Naples, Italy; orcid.org/0000-0002-0169-4441; Email: valentina.sepe@unina.it

Authors

Bianca Fiorillo – Department of Pharmacy, University of Naples “Federico II”, I-80131 Naples, Italy; orcid.org/0000-0002-3025-5157

Rosalinda Roselli – Department of Pharmacy, University of Naples “Federico II”, I-80131 Naples, Italy
Claudia Finamore – Department of Pharmacy, University of Naples “Federico II”, I-80131 Naples, Italy
Cristina di Giorgio – Department of Medicine and Surgery, University of Perugia, I-06132 Perugia, Italy
Martina Bordoni – Precision BioTherapeutics, Srl, Perugia 06128, Italy
Paolo Conflitti – Faculty of Biomedical Sciences, Euler Institute, Università della Svizzera italiana (USI), CH-6900 Lugano, Switzerland
Silvia Marchianò – Department of Medicine and Surgery, University of Perugia, I-06132 Perugia, Italy
Rachele Bellini – Department of Medicine and Surgery, University of Perugia, I-06132 Perugia, Italy
Pasquale Rapacciuolo – Department of Pharmacy, University of Naples “Federico II”, I-80131 Naples, Italy
Chiara Cassiano – Department of Pharmacy, University of Naples “Federico II”, I-80131 Naples, Italy
Vittorio Limongelli – Department of Pharmacy, University of Naples “Federico II”, I-80131 Naples, Italy; Faculty of Biomedical Sciences, Euler Institute, Università della Svizzera italiana (USI), CH-6900 Lugano, Switzerland; orcid.org/0000-0002-4861-1199
Bruno Catalanotti – Department of Pharmacy, University of Naples “Federico II”, I-80131 Naples, Italy; orcid.org/0000-0002-7532-6959
Stefano Fiorucci – Department of Medicine and Surgery, University of Perugia, I-06132 Perugia, Italy
Angela Zampella – Department of Pharmacy, University of Naples “Federico II”, I-80131 Naples, Italy; orcid.org/0000-0002-6170-279X

Complete contact information is available at:
<https://pubs.acs.org/10.1021/acsomega.2c07907>

Author Contributions

¹B.F., R.R., and C.F. contributed equally. The manuscript was written through contributions of all authors. All authors have given approval to the final version of the manuscript.

Notes

The authors declare the following competing financial interest(s): S. F. and A. Z. have filed a patent application in the name of PRECISION BIO-THERAPEUTICS S.R.L., a spinoff of the University of Perugia, on the same compounds described in this paper.

ACKNOWLEDGMENTS

This work was partially supported by a grant from the University of Naples Federico II “Finanziamento della Ricerca in Ateneo,” Linea B-Project MoDiGa and by a grant from the Italian MIUR/PRIN 2017 (2017FJZZRC). V.L. acknowledges the support from the European Research Council (“CoMMBi” ERC grant agreement No. 101001784) and the Swiss National Supercomputing Centre (CSCS) [project ID s1150].

REFERENCES

- (1) Ridlon, J. M.; Kang, D.-J.; Hylemon, P. B. Bile Salt Biotransformations by Human Intestinal Bacteria. *J. Lipid Res.* **2006**, *47*, 241–259.
- (2) Fiorucci, S.; Carino, A.; Baldoni, M.; Santucci, L.; Costanzi, E.; Graziosi, L.; Distrutti, E.; Biagioli, M. Bile Acid Signaling in Inflammatory Bowel Diseases. *Dig. Dis. Sci.* **2021**, *66*, 674–693.
- (3) Chiang, J. Y. L. Bile Acids: Regulation of Synthesis. *J. Lipid Res.* **2009**, *50*, 1955–1966.
- (4) Makishima, M.; Okamoto, A. Y.; Repa, J. J.; Tu, H.; Learned, R. M.; Luk, A.; Hull, M. V.; Lustig, K. D.; Mangelsdorf, D. J.; Shan, B. Identification of a Nuclear Receptor for Bile Acids. *Science* **1999**, *284*, 1362–1365.
- (5) Biagioli, M.; Carino, A.; Fiorucci, C.; Marchianò, S.; di Giorgio, C.; Roselli, R.; Magro, M.; Distrutti, E.; Bereshchenko, O.; Scarpelli, P.; Zampella, A.; Fiorucci, S. GPBAR1 Functions as Gatekeeper for Liver NKT Cells and Provides Counterregulatory Signals in Mouse Models of Immune-Mediated Hepatitis. *Cell Mol. Gastroenterol. Hepatol.* **2019**, *8*, 447–473.
- (6) Zwicky, P.; Unger, S.; Becher, B. Targeting Interleukin-17 in Chronic Inflammatory Disease: A Clinical Perspective. *J. Exp. Med.* **2020**, *217*, e20191123.
- (7) Jetten, A. M. Retinoid-Related Orphan Receptors (RORs): Critical Roles in Development, Immunity, Circadian Rhythm, and Cellular Metabolism. *Nucl. Recept. Signal.* **2009**, *7*, No. nrs.07003.
- (8) Sun, Z.; Unutmaz, D.; Zou, Y.-R.; Sunshine, M. J.; Pierani, A.; Brenner-Morton, S.; Mebius, R. E.; Littman, D. R. Requirement for ROR γ in Thymocyte Survival and Lymphoid Organ Development. *Science* **2000**, *288*, 2369–2373.
- (9) Ivanov, I. I.; McKenzie, B. S.; Zhou, L.; Tadokoro, C. E.; Lepelley, A.; Lafaille, J. J.; Cua, D. J.; Littman, D. R. The Orphan Nuclear Receptor ROR γ t Directs the Differentiation Program of Proinflammatory IL-17+ T Helper Cells. *Cell* **2006**, *126*, 1121–1133.
- (10) Burris, T. P.; Busby, S. A.; Griffin, P. R. Targeting Orphan Nuclear Receptors for Treatment of Metabolic Diseases and Autoimmunity. *Chem. Biol.* **2012**, *19*, 51–59.
- (11) Zhang, Y.; Luo, X.; Wu, D.; Xu, Y. ROR Nuclear Receptors: Structures, Related Diseases, and Drug Discovery. *Acta Pharmacol. Sin.* **2015**, *36*, 71–87.
- (12) Jetten, A. M.; Takeda, Y.; Slominski, A.; Kang, H. S. Retinoic Acid-Related Orphan Receptor γ (ROR γ): Connecting Sterol Metabolism to Regulation of the Immune System and Autoimmune Disease. *Curr. Opin. Toxicol.* **2018**, *8*, 66–80.
- (13) Solt, L. A.; Kumar, N.; Nuhant, P.; Wang, Y.; Lauer, J. L.; Liu, J.; Istrate, M. A.; Kamenecka, T. M.; Roush, W. R.; Vidović, D.; Schürer, S. C.; Xu, J.; Wagoner, G.; Drew, P. D.; Griffin, P. R.; Burris, T. P. Suppression of TH17 Differentiation and Autoimmunity by a Synthetic ROR Ligand. *Nature* **2011**, *472*, 491–494.
- (14) Wang, Y.; Kumar, N.; Crumbley, C.; Griffin, P. R.; Burris, T. P. A Second Class of Nuclear Receptors for Oxysterols: Regulation of ROR α and ROR γ Activity by 24S-Hydroxycholesterol (Cerebrosterol). *Biochim. Biophys. Acta Mol. Cell Biol. Lipids* **2010**, *1801*, 917–923.
- (15) Huh, J. R.; Leung, M. W. L.; Huang, P.; Ryan, D. A.; Krout, M. R.; Malapaka, R. R. v.; Chow, J.; Manel, N.; Ciofani, M.; Kim, S.; Cuesta, A.; Santori, F. R.; Lafaille, J. J.; Xu, H. E.; Gin, D. Y.; Rastinejad, F.; Littman, D. R. Digoxin and Its Derivatives Suppress TH17 Cell Differentiation by Antagonizing ROR γ t Activity. *Nature* **2011**, *472*, 486–490.
- (16) Fujita-Sato, S.; Ito, S.; Isobe, T.; Ohyama, T.; Wakabayashi, K.; Morishita, K.; Ando, O.; Isono, F. Structural Basis of Digoxin That Antagonizes ROR γ t Receptor Activity and Suppresses Th17 Cell Differentiation and Interleukin (IL)-17 Production. *J. Biol. Chem.* **2011**, *286*, 31409–31417.
- (17) Kallen, J.; Izaac, A.; Be, C.; Arista, L.; Orain, D.; Kaupmann, K.; Guntermann, C.; Hoegenauer, K.; Hintermann, S. Structural States of ROR γ t: X-Ray Elucidation of Molecular Mechanisms and Binding Interactions for Natural and Synthetic Compounds. *ChemMedChem* **2017**, *12*, 1014–1021.
- (18) Noguchi, M.; Nomura, A.; Doi, S.; Yamaguchi, K.; Hirata, K.; Shiozaki, M.; Maeda, K.; Hirashima, S.; Kotoku, M.; Yamaguchi, T.; Katsuda, Y.; Crowe, P.; Tao, H.; Thacher, S.; Adachi, T. Ternary Crystal Structure of Human ROR γ Ligand-Binding-Domain, an Inhibitor and Corepressor Peptide Provides a New Insight into Corepressor Interaction. *Sci. Rep.* **2018**, *8*, No. 17374.

- (19) Fauber, B. P.; Magnuson, S. Modulators of the Nuclear Receptor Retinoic Acid Receptor-Related Orphan Receptor- γ (ROR γ or RORc). *J. Med. Chem.* **2014**, *57*, 5871–5892.
- (20) Keitel, V.; Donner, M.; Winandy, S.; Kubitz, R.; Häussinger, D. Expression and Function of the Bile Acid Receptor TGR5 in Kupffer Cells. *Biochem. Biophys. Res. Commun.* **2008**, *372*, 78–84.
- (21) Klepsch, V.; Moschen, A. R.; Tilg, H.; Baier, G.; Hermann-Kleiter, N. Nuclear Receptors Regulate Intestinal Inflammation in the Context of IBD. *Front. Immunol.* **2019**, *10*, 1070.
- (22) Mickael, M. E.; Bhaumik, S.; Basu, R. Retinoid-Related Orphan Receptor ROR γ t in CD4+ T-Cell-Mediated Intestinal Homeostasis and Inflammation. *Am. J. Pathol.* **2020**, *190*, 1984–1999.
- (23) Sun, N.; Yuan, C.; Ma, X.; Wang, Y.; Gu, X.; Fu, W. Molecular Mechanism of Action of ROR γ t Agonists and Inverse Agonists: Insights from Molecular Dynamics Simulation. *Molecules* **2018**, *23*, 3181.
- (24) Biagioli, M.; Marchianò, S.; Carino, A.; di Giorgio, C.; Santucci, L.; Distrutti, E.; Fiorucci, S. Bile Acids Activated Receptors in Inflammatory Bowel Disease. *Cells* **2021**, *10*, 1281.
- (25) Gege, C. Retinoic Acid-Related Orphan Receptor Gamma t (ROR γ t) Inverse Agonists/Antagonists for the Treatment of Inflammatory Diseases – Where Are We Presently? *Expert Opin. Drug Discovery* **2021**, *16*, 1517–1535.
- (26) Sepe, V.; Ummano, R.; D'Auria, M. V.; Mencarelli, A.; D'Amore, C.; Renga, B.; Zampella, A.; Fiorucci, S. Total Synthesis and Pharmacological Characterization of Solomonsterol A, a Potent Marine Pregnane-X-Receptor Agonist Endowed with Anti-Inflammatory Activity. *J. Med. Chem.* **2011**, *54*, 4590–4599.
- (27) Terasawa, T.; Ikekawa, N.; Morisaki, M. Photochemical Reaction of Cholesterol Analogs with a Carbene-Generating Substituent on the Side Chain. *Chem. Pharm. Bull.* **1986**, *34*, 935–936.
- (28) Averin, A. D.; Ranyuk, E. R.; Lukashev, N. V.; Beletskaya, I. P. Synthesis of Nitrogen- and Oxygen-Containing Macrocycles—Derivatives of Lithocholic Acid. *Chem. Eur. J.* **2005**, *11*, 7030–7039.
- (29) Anzini, M.; Braile, C.; Valenti, S.; Cappelli, A.; Vomero, S.; Marinelli, L.; Limongelli, V.; Novellino, E.; Betti, L.; Giannaccini, G.; Lucacchini, A.; Ghelardini, C.; Norcini, M.; Makovec, F.; Giorgi, G.; Ian Fryer, R. Ethyl 8-Fluoro-6-(3-Nitrophenyl)-4 H -Imidazo[1,5- a][1,4]-Benzodiazepine-3-Carboxylate as Novel, Highly Potent, and Safe Antianxiety Agent. *J. Med. Chem.* **2008**, *51*, 4730–4743.
- (30) Anzini, M.; Valenti, S.; Braile, C.; Cappelli, A.; Vomero, S.; Alcaro, S.; Ortuso, F.; Marinelli, L.; Limongelli, V.; Novellino, E.; Betti, L.; Giannaccini, G.; Lucacchini, A.; Daniele, S.; Martini, C.; Ghelardini, C.; di Cesare Mannelli, L.; Giorgi, G.; Mascia, M. P.; Biggio, G. New Insight into the Central Benzodiazepine Receptor–Ligand Interactions: Design, Synthesis, Biological Evaluation, and Molecular Modeling of 3-Substituted 6-Phenyl-4 H -Imidazo[1,5- a][1,4]-Benzodiazepines and Related Compounds. *J. Med. Chem.* **2011**, *54*, 5694–5711.
- (31) Deplano, A.; Morgillo, C. M.; Demurtas, M.; Björklund, E.; Cipriano, M.; Svensson, M.; Hashemian, S.; Smaldone, G.; Pedone, E.; Luque, F. J.; Cabiddu, M. G.; Novellino, E.; Fowler, C. J.; Catalanotti, B.; Onnis, V. Novel Propanamides as Fatty Acid Amide Hydrolase Inhibitors. *Eur. J. Med. Chem.* **2017**, *136*, 523–542.
- (32) *Glide, Version 7.1*; Schrödinger, LLC: New York, NY, 2019.
- (33) Jin, L.; Martynowski, D.; Zheng, S.; Wada, T.; Xie, W.; Li, Y. Structural Basis for Hydroxycholesterols as Natural Ligands of Orphan Nuclear Receptor ROR γ . *Mol. Endocrinol.* **2010**, *24*, 923–929.
- (34) D'Amore, C.; di Leva, F. S.; Sepe, V.; Renga, B.; del Gaudio, C.; D'Auria, M. V.; Zampella, A.; Fiorucci, S.; Limongelli, V. Design, Synthesis, and Biological Evaluation of Potent Dual Agonists of Nuclear and Membrane Bile Acid Receptors. *J. Med. Chem.* **2014**, *57*, 937–954.
- (35) Biagioli, M.; Carino, A.; Cipriani, S.; Francisci, D.; Marchianò, S.; Scarpelli, P.; Sorcini, D.; Zampella, A.; Fiorucci, S. The Bile Acid Receptor GPBAR1 Regulates the M1/M2 Phenotype of Intestinal Macrophages and Activation of GPBAR1 Rescues Mice from Murine Colitis. *J. Immunol.* **2017**, *199*, 718–733.
- (36) Festa, C.; Renga, B.; D'Amore, C.; Sepe, V.; Finamore, C.; de Marino, S.; Carino, A.; Cipriani, S.; Monti, M. C.; Zampella, A.; Fiorucci, S. Exploitation of Cholane Scaffold for the Discovery of Potent and Selective Farnesoid X Receptor (FXR) and G-Protein Coupled Bile Acid Receptor 1 (GP-BAR1) Ligands. *J. Med. Chem.* **2014**, *57*, 8477–8495.
- (37) Huh, J. R.; Englund, E. E.; Wang, H.; Huang, R.; Huang, P.; Rastinejad, F.; Inglese, J.; Austin, C. P.; Johnson, R. L.; Huang, W.; Littman, D. R. Identification of Potent and Selective Diphenylpropanamide ROR γ Inhibitors. *ACS Med Chem Lett.* **2013**, *4*, 79–84.
- (38) Thibaut, M. M.; Bindels, L. B. Crosstalk between Bile Acid-Activated Receptors and Microbiome in Entero-Hepatic Inflammation. *Trends Mol. Med.* **2022**, *28*, 223–236.
- (39) Song, X.; Sun, X.; Oh, S. F.; Wu, M.; Zhang, Y.; Zheng, W.; Geva-Zatorsky, N.; Jupp, R.; Mathis, D.; Benoist, C.; Kasper, D. L. Microbial Bile Acid Metabolites Modulate Gut ROR γ + Regulatory T Cell Homeostasis. *Nature* **2020**, *577*, 410–415.